CSCE Annual Conference

Growing with youth – Croître avec les jeunes

Laval (Greater Montreal)

June 12 - 15, 2019

INVESTIGATION ON THE FLEXURAL CAPACITY OF ULTRA-HIGH PERFORMANCE FIBRE REINFORCED CONCRETE BEAMS

Madanat, J.[1,3], Othman, H.[2], Marzouk, H.[2]

[1] M.A.Sc. Candidate at Ryerson University, Canada

[2] Faculty of Engineering & Architectural Science, Ryerson University, Canada

[3] jalimdan@ryerson.ca

Abstract: Ultra-high performance fibre reinforced concrete (UHPFRC) is a relatively new generation of cementitious material that exhibits exceptional mechanical and durability characteristics in comparison to its traditional counterparts. Despite the obvious advantage of UHPFRC, its structural application is not widespread. One of the main reasons that have delayed the extensive use of UHPFRC has been the lack of widely accepted building code design guidelines. Additionally, the flexural (moment) capacity of UHPFRC beams is an ongoing task for researchers. This task is complicated due to the presence of steel fibres in the specimen which shifts the neutral axis location. The inclusion of these fibres is not incorporated into traditional reinforced concrete design guidelines. Thus, current design codes could not provide an accurate estimation of the moment capacity of UHPFRC structural members. In this investigation, five specimens are tested under incremental flexural loads to failure and the capacities of all tested specimens are estimated analytically using different design standards like the ACI 318-02, CSA A23.3-94, NZS 3101-1995, French Model, Bae et al., and the Ryerson Proposed Method (RPM). The goal is to achieve a moment capacity with a closer range than the current American (ACI) and Canadian (CSA) standards that provide only 76% of the actual capacity as reported in previous literature.

1 INTRODUCTION

Ultra-high performance fibre reinforced concrete (UHPFRC) is a new promising material that exhibits superior strength, ductility and durability properties over conventional concrete. New advances in concrete materials and behaviours is an ongoing journey for engineers and researchers. UHPFRC is an advanced material that has undergone significant research in the past few decades. The most favourable aspects of this material are superior mechanical properties and improved durability. UHPFRC has a compressive strength greater than 150 MPa (Wille & Naaman, 2012) in addition to high tensile strength. Moreover, it has high fracture energy (Othman & Marzouk, 2018), post-cracking strength (Kim et al., 2009) and dimensional stability. UHPFRC has been identified as one of the promising ways to innovate in impact resistance structures. Despite the obvious advantage of UHPFRC mechanical and durability properties, its structural application is not very widespread.

In this investigation, five UHPFRC beams are constructed and tested experimentally. The experimental results are used to calibrate the analytical models. Moreover, different mechanical properties such as compressive strength and fracture energy will be presented herein.

2 MECHANICAL PROPERTIES

Several investigations have shown that the mechanical properties of UHPFRC material are different from traditional concrete, in particular, the tensile response and fracture energy. In addition, UHPFRC shows improved durability which makes it favourable to use in aggressive environments (Chahrron et al., 2006). Moreover, ductility is greatly enhanced with the inclusion of steel fibres (Wille et al., 2010). The aforementioned properties of UHPFRC make it a superior material over conventional concrete. Table 1 summarizes the main mechanical properties of UHPFRC with a fibre volume content of 2%.

Table 1: Mechanical Properties of UHPFRC (Othman & Marzouk, 2018)

Density	2650 kg/m^3
Compressive strength f_c'	162.4 MPa
Strain at peak stress ϵ_o	4.0 x 10^{-3}
Elastic modulus E_c	48.8 MPa
Splitting strength f_{tsp}	11.1 GPa
Flexural strength f_r	19.2 MPa
Fracture energy G_F	17985 N/m

2.1 Compressive Strength

The compressive strength of three types of concrete was measured using fibre optic sensors at Ryerson University (Othman & Marzouk, 2016) for normal, high strength and UHPFRC. Three sets of cylinders (100x200mm) were prepared and tested in order to obtain various mechanical properties of concrete of each type. Three cylinders were prepared for each type with FBG (fibre Bragg grating) sensors for each type of concrete in order to capture the strain and elastic modulus. These sensors were embedded in the middle centre of the cylinders as shown in Figure 1. The rest of the cylinders were tested under compression to obtain the 28-day compressive strength. All cylinders were tested using an MTS machine due to its ability to control the desired loading rate. The cylinders were moist cured for 28 days prior to testing.

Figure 1: Cylinders equipped with FBG sensors (left) and the MTS machine used for testing (right) (Othman & Marzouk, 2016)

The UHPFRC cylinders that were tested for compression had an average strength of 163 MPa after 28 days of moist curing. The elastic modulus for the UHPFRC with 2% steel fibres is 48.8 GPa (Othman, 2016). The axial strains for high strength concrete (HSC) and UHPFRC with 2% fibre volume developed at Ryerson University by Yazdizadeh (2014) and Othman (2016) are shown in Figure 2. The original testing was done by Yazdizadeh (2014). Furthermore, a new stress block is idealized as shown by Figure 2 with a strain of 0.0035 and 0.005 at the maximum stress, along with an ultimate descending strain of 0.008 (Othman, 2016).

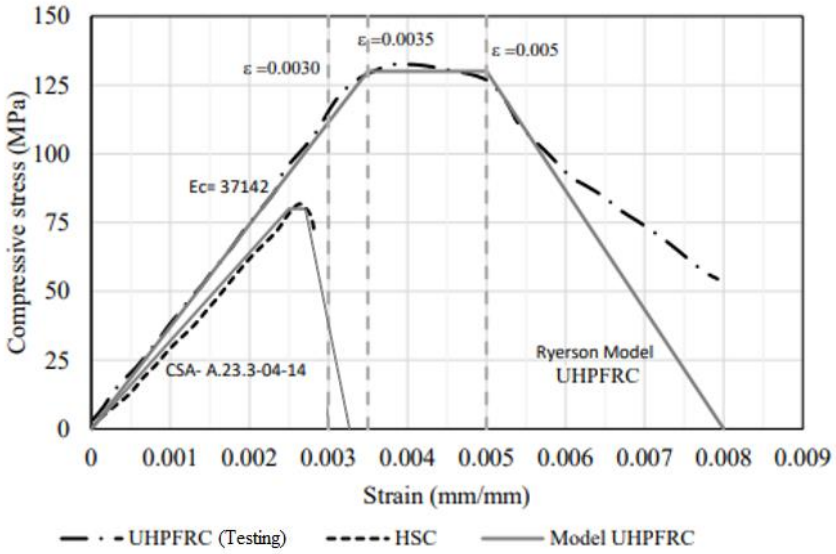

Figure 2: Axial strain vs compressive stress for HSC & UHPFRC (Yazdizadeh, 2014)

2.2 Fracture Energy

Fracture energy is another important concept that is peculiar to UHPFRC. The higher the fracture energy, the higher the ductility and failure capacity.

Both strain hardening and strain softening UHPFRC are presented by a model for predicting bending behaviour as recommended by the French code (Figure 3). The model is based on a modified force-based fibre-beam formulation where progressive loading is driven by curvature at its non-linear hinge.

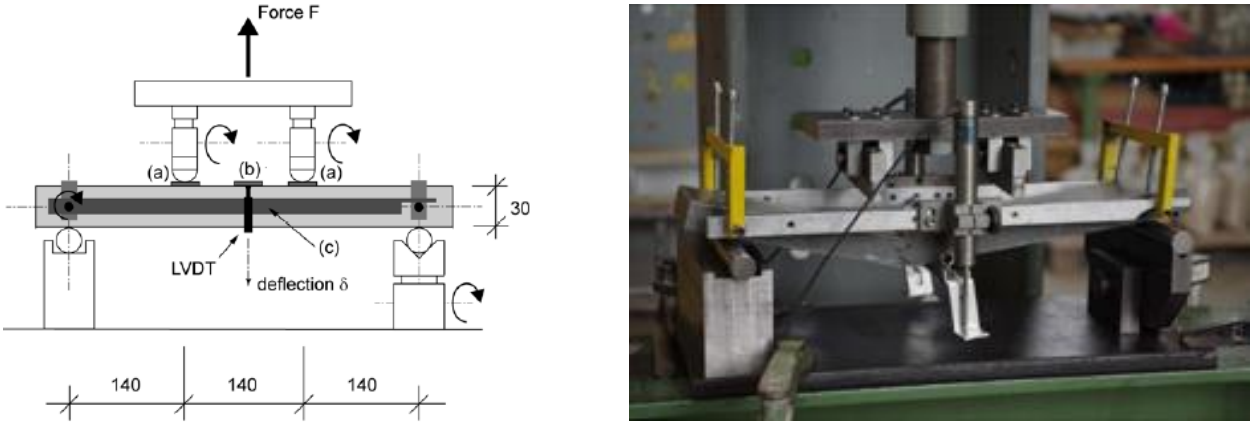

Figure 3: Four-point bending set-up according to the French code (Dobrusky, 2017)

According to the experimental testing at Ryerson by Wahba (2012), the fracture energy of UHPFRC with 2% fibres is 100 times that of traditional concrete (Table 2). This is confirmed more recently by Maca et al. (2013) and Othman and Marzouk (2018) who validated the results by inverse analysis using numerical simulation.

Table 2: Tension and Fracture Properties of UHPFRC (Wahba, 2012)

Specimen Name	f_c' (MPa)	f_u (kN)	ϵ_p x 10^{-6}	G_F (N/m)	E_t (GPa)	f_r (MPa)
FE1	163	100.25	3500	18,839.4	58	8.68
FE2	137	97.5	2700	16,852.4	57	8.44

Figure 4 shows the fracture energy dissipation for strain hardening and softening material. As can be seen, strain hardening is characterized by multiple cracking as opposed to strain softening which allows for the development of one crack (Xu & Wille, 2015). In addition, the fracture energy dissipation for strain hardening is bigger than for softening. UHPFRC undergoes four distinct stages from the point of loading until complete failure. These stages include linear elastic, strain hardening, followed by softening, then complete failure (Naaman, 2008). These distinct stages are unique to UHPFRC and are not found in normal or high strength concrete.

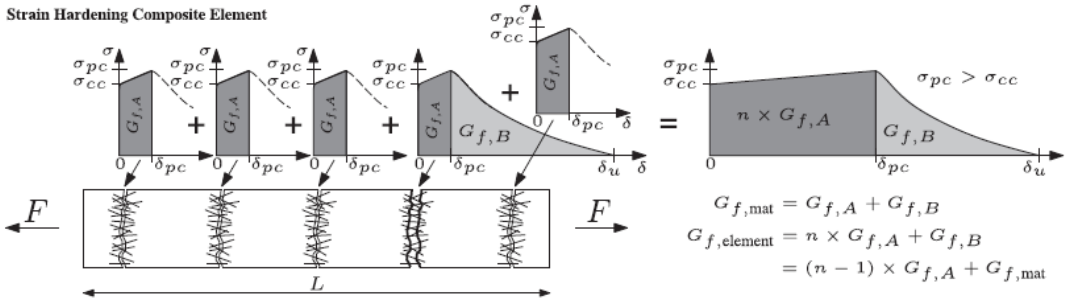

Figure 4: Fracture energy for strain hardening and softening (Xu & Wille, 2015)

3 EXPERIMENTAL PROCEDURE

3.1 Test Specimens Preparation

The mixing was performed twice; once for the 2 long span beams and the second for the 3 short span beams. After the first concrete mix procedure, the concrete was carried by a bucket and transported to two wooden beam formwork (molds) with a cross-sectional area of 178mm x 305mm (long span beams). Following the second mix procedure, the concrete was cast into three molds with a cross-sectional area of 178mm x 305mm (short span beams). In addition, a 10mm strain gauge was placed in the middle of the steel rebar to measure the reinforcing steel strain during testing. In this investigation, 5 beams were constructed, according to Table 3.

Table 3: Specification of test specimens

Specimen Name	Span, L (mm)	Cross Section (mm^2)	Span to Depth Ratio, L/d	Compressive Strength*, f_c' (MPa)	Steel Ratio, p_w
2-20M-S	915	178x305	3.5	163	0.0127
4-20M-S	915		3.5		0.0254
6-20M-S	915		3.6		0.040
6-20M-L	1830		7.3		0.040
8-20M-L**	1830		6.9&45.8		0.0254&0.169

*Average value

**Doubly reinforced

3.2 Test Specimens Procedure

The testing procedure for all five beams was performed using a loading frame with a hydraulic jack that applies load increments on the test specimen as shown in Figure 5. The hydraulic jack along with the strain gauge were connected to a data acquisition system. Moreover, a linear variable differential transformer (LVDT) was placed in the middle of the beams to capture the mid-span displacement. All five beams were tested under four-point loading with an initial load increment of 20 kN. This increment was later increased to 30 kN to minimize the testing duration due to the superior concrete strength of UHPFRC.

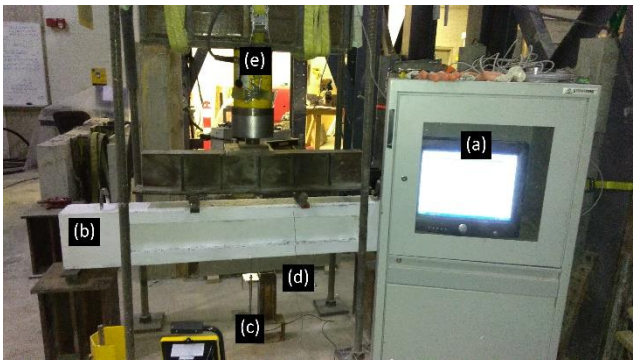

(a) Acquisition system

(b) Test specimen

(c) LVDT

(d) Strain gauge wire

(e) Test Apparatus

Figure 5: Test setup and instrumentation

3.3 Test Results and Discussion

Conventional concrete is a brittle material which makes it difficult to capture the complete load-deformation graph. This issue can be resolved with UHPFRC which contain steel fibres that enhance the ductility of concrete allowing it to undergo strain hardening and softening which is evident in the ascending and descending portions of the graph as shown in Figure 4.

Before surface cracks appeared, multiple internal cracks occurred in the concrete. They were prevented from propagating to the surface since steel fibres were used. Steel fibres play an important part in improving ductility because they bridge the gap between the cracks. However, this is not the case with conventional concrete due to the absence of steel fibres, which facilitate the quick emergence of internal cracks to the surface causing failure to occur much faster and at a lower loading.

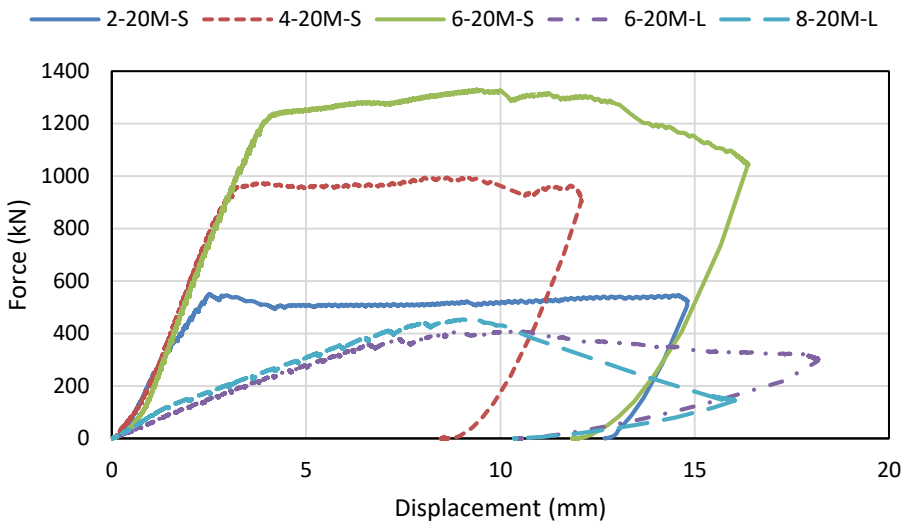

Figure 6: Load-displacement of UHPFRC beams (S = 915mm beam, L = 1830mm beam)

Figure 6 shows various failure loads reached by each beam along with the maximum mid-span displacement. It's interesting to note the wide gap between the ascending and descending branches for each specimen. This indicates that multiple cracks occurred after the linear elastic region and before complete failure. This is a favourable aspect of UHPFRC as it allows the material to undergo larger than usual deformation before failure.

4 FLEXURAL BEHAVIOUR OF REINFORCED UHPFRC BEAMS

There is a lot of ongoing research on UHPFRC in order to determine its behaviour and characteristics. One area of interest that should be examined is the flexural capacity of UHPFRC. There is a lot of research and codes on the moment capacity of normal strength concrete. However, design codes lack proper formulas and procedure for UHPFRC. The procedure for calculating the moment capacity of UHPFRC is complicated by the presence of steel fibres in the concrete that induces additional tensile forces not found or regarded in conventional concrete. These additional tensile forces due to steel fibres shift the location of the neutral axis which makes standard codes and procedures obsolete for obtaining proper and accurate flexural capacities. Previous research on UHPFRC prestressed I-girders found the moment capacity to be 76% of the experimental results using the Whitney stress block (Graybeal, 2008). Other research has been attempted to minimize the difference between the numerical and experimental values such as Singh et al., (2017).

The following sections look at different analytical methods for calculating the moment capacity of UHPFRC beams. The results of these methods are reported at the end of this section in Tables 4 and 5.

4.1 Beam Flexure Analysis

Bae et al., (2016) investigated the stress block of nine different types of flexural strength models and recommended the following stress block shown in Figure 7. Calculating the moment capacity for UHPFRC is different than for conventional concrete. The authors put the nine different types to the test by comparing the flexural capacities that they produced with the experimental model. The researchers proposed a new stress block for calculating the neutral axis depth and obtaining the moment capacity for UHPFRC. It was shown that the stress block in Figure 7 produced the closest capacity to the experimental model. The trick to achieving better results with UHPFRC is the inclusion of steel fibres in the model. Moreover, it's crucial to use the right stress block parameters. The stress block in Figure 7 was effective because it used a triangular distribution in compression to account for the steel fibres. The following two equations (Eq.1 and

Eq.2) presented below are used in this method to calculate the neutral axis location and the moment capacity. It's worth noting some of the variables in these equations. The gamma γ term used here is the ratio between post cracking and ultimate tensile strengths. Through trial and error, it was observed that a gamma value of 0.7 yields the best results. Moreover, f_t, the tensile strength of the concrete is taken as 9% of the compressive strength (9% of 163 MPa; 14.7 MPa). The α and β terms for UHPFRC are taken as 0.85 & 0.65, respectively (Graybeal, 2008). The width (b) and height (h) of the beam specimen are 178mm x 305mm. Moreover, f_c' is the concrete compressive strength (163 MPa), f_y the yield strength of reinforcing steel (400 MPa), A_s is the area of flexural reinforcement, η is a ratio between the ultimate tensile and compressive concrete strains plus one (taken as 1.4), and d is the effective depth measured from the top compression fibre to the centroid of main flexural steel bars. Numerical results for different reinforcements are presented in Tables 4 and 5.

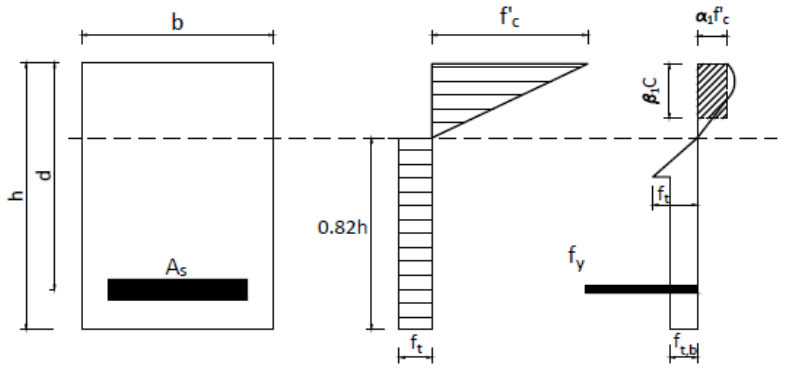

α_1 , β_1 are rectangular stress block parameters.

f'_c , f_t are compressive and tensile strengths of concrete, respectively

f_y is the yield strength of concrete

h, b are the cross-sectional dimensions and d is the effective depth

A_s is the area of flexural reinforcement

Figure 7: Stress block models for French code (centre) and Bae et al. (right) (Bae et al., 2016, Dobrusky, 2017)

[1] $C = \frac{A_s f_y + \gamma f_t b h}{\alpha_1 f_c' \beta_1 b - 0.5(\eta-1) f_t b + \gamma \eta f_t b}$ Bae et al., (2016)

[2] $M = (\alpha_1 f_c' \beta_1 c b)(\frac{c}{2}) + \{f_t(e-c)b\}(\frac{2}{3})(e-c) + \{\gamma f_t(h-e)b\}(e-c+\frac{h-e}{c}) + A_s f_y(d-c)$ Bae et al., (2016)

Where,

$e = (e_{sfibers} + 0.003)(c/0.003)$, c being the neutral axis depth and $e_{sfibers}$ is taken as 0.0036.

4.2 Ryerson Proposed Method (RPM)

Another method used in this report for obtaining the flexural capacity of reinforced concrete beams is a proposed method that is formulated at Ryerson University. The rationale behind the method is to assume that the compression depth of the stress block is the same as the neutral axis depth; which means that β_1 is simply one. The following procedure locates the neutral axis depth of the beams. After assuming that β_1 is one, the next step is to calculate the moment about the neutral axis by substituting a variable (x) in place of a (neutral axis depth) in the compression force equation. This is done by equating the compression force with the tension force in the flexural steel and the force in the steel fibres (which is approximately in the middle of the tension side of the stress block). This is done for the plain beam as well as the 2-20M, 4-20M, 6-20M, and 8-20M specimen.

4.3 French Model (Dobrusky, 2017)

The other method used in this report to obtain flexural capacity is a French model proposed by Dobrusky (2017). This French model proposed by Dobrusky is unique because it saves computational time as it works directly in the moment-curvature space. This process saves computational time and cost associated with

section integration that is usually performed in the fibre-beam model (Dobrusky, 2017). Dobrusky's proposed model reduces the computation to one numerical loop (Dobrusky, 2017). Moreover, this model assumes that the neutral axis location (0.18*h) is the same for the plain and reinforced beams (Figure 7). Dobrusky's proposed force equation for point "C" between strain hardening and softening is:

[3] $F_c = \frac{f_t.b.h^2}{0.383.L}$ Dobrusky (2017)

F_t (maximum tensile strength) is the maximum stress at point C and is 9% of the concrete compressive strength (163 MPa). The terms "b" and "h" are the section dimensions (178x305mm), while L is the span of the beam. The moment capacity of the plain unreinforced beam was found to be:

[4] $M = F.d,$

Where d is the moment arm between the compression/tension centroids. The capacity of the reinforced beams was the summation of the aforementioned moment and $A_s f_y d$, where f_y is the yield strength of steel (400 MPa) and A_s the area of the flexural rebars.

4.4 CSA A23.3-94/ ACI 318-02/ NZS 3101-1995

CSA A23.3-94, ACI 318-02, and the NZS 3101-1995 design codes are formulated for traditional concrete that has low compressive strength and almost negligible tensile strength. Therefore, since UHPFRC has superior compressive and tensile strengths over traditional concrete, these codes are not applicable for determining the flexural capacity of UHPFRC beams as is evident in Tables 4 and 5. Moreover, the exclusion of the effect of steel fibres in these design codes is another factor for the low flexural capacity.

4.5 Moment Capacity Comparison Between Experimental and Analytical Methods

This section presents a summary of the moment capacity values obtained using the analytical methods for the various tested specimen and compares it against the experimental capacities. These results are summarized in Tables 4 and 5. It should be noted that the α which was used in calculating the moment capacities is the 0.85 suggested by Graybeal (2008). A new α value was proposed (RPM) but that value (0.56) did not change the moment capacity value (~5% difference).

Table 4: Comparison of moment capacity for specimen span 915mm

Method	2-20M Moment capacity (kN.m)	4-20M Moment capacity (kN.m)	6-20M Moment capacity (kN.m)
Bae et al.	133.3	186.1	226.6
French Model	171.5	230.7	280.3
RPM	134.2	189.5	233.1
ACI 318-02	62.4	122.5	170.7
CSA A23.3-94	62.0	120.6	166.5
NZS 3101-1995	61.2	118.0	160.0
Experimental	170.5	308.5	412.4
Moment comparison for:			
Bae et al.	78.2%	60.3%	54.9%
French Model	100.6%	74.8%	68.0%
RPM	78.7%	61.4%	56.5%
ACI 318-02	36.6%	39.7%	41.4%
CSA A23.3-94	36.4%	39.1%	40.4%
NZS 3101-1995	35.9%	38.2%	38.8%

Table 5: Comparison of moment capacity for specimen span 1830mm

Method	Plain/Unreinforced Moment capacity (kN.m)	2-20M Moment capacity (kN.m)	4-20M Moment capacity (kN.m)	6-20M Moment capacity (kN.m)	8-20M Moment capacity (kN.m)
Bae et al.	77.6	133.3	186.1	226.6	217.7
French Model	56.2	115.4	174.6	224.2	185.0
RPM	76.6	134.2	189.5	233.1	185.6
ACI 318-02	62.4	62.4	122.5	170.7	108.0
CSA A23.3-94	62.0	62.0	120.6	166.5	108.0
NZS 3101-1995	61.2	61.2	118.0	160.0	108.0
Experimental	54.9*	143.4*	201.3*	249.7	277.2
Moment comparison for:					
Bae et al.	141.3%	93.0%	92.4%	90.7%	78.5%
French Model	102.4%	80.5%	86.7%	89.8%	66.7%
RPM	139.5%	93.6%	94.1%	93.4%	67.0%
ACI 318-02	113.7%	43.5%	60.9%	68.4%	39.0%
CSA A23.3-94	112.9%	43.2%	59.9%	66.7%	39.0%
NZS 3101-1995	111.5%	42.7%	58.6%	64.1%	39.0%

*Values from previous literature (Wahba, 2012, pp. 61)

5 CONCLUSION

UHPFRC is a promising material that is used in multiple applications where enhanced durability and strength are required due to its superior mechanical properties. The focus of this paper has been on the flexural capacity of UHPFRC beams where different codes and methods were presented and compared with experimental results. The following conclusions can be drawn from this research:

- Design guidelines such as ACI 318-02/CSA A23.3-94/NZS 3101-1995 using Whitney's stress block are not suitable for the design of UHPFRC beams due to their low accuracy as can be seen in Tables 4 and 5. Two important reasons for this low accuracy are the lack of inclusion of steel fibres and the effect of the tensile strength of concrete in traditional building codes.
- Both Ryerson Proposed Method (RPM) and Bae et al. (2016) show great accuracy for long span specimen (1830mm), followed by the French model presented by Dobrusky (2017).
- RPM, French model, and Bae at al. (2016) are not suitable for the short, bulky specimen (915mm). Perhaps a strut and tie model could be used for such a specimen.
- Overall, the method proposed by Bae at al. (2016) gives the highest accuracy for long span specimen.

Acknowledgements

The first author would like to acknowledge Dr. Marzouk and Dr. Othman for their guidance and assistance; their support is greatly appreciated. Moreover, the author would like to thank Lafarge North America for their support in providing concrete dry materials. In addition, the support of Mr. Jaalouk and the technical staff at Ryerson University is kindly appreciated.

References

Bae, B.I., Choi, H.K. and Choi, C.S. 2015. Flexural Strength Evaluation of Reinforced Concrete Members with Ultra High Performance Concrete. *Advances in Materials Science and Engineering*: 1-10.

Charron, J.P., Denarie, E. and Bruhwiler, E. 2007. Permeability of Ultra High Performance Fiber Reinforced Concretes (UHPFRC) Under High Stresses. *Materials and Structures*, **40**: 269-277.

Dobrusky, S. 2017. Inverse Analysis Tailored for Both Strain Hardening and Strain Softening UHPFRC. *Int. Symposium on Ultra-High Performance Fibre-Reinforced Concrete*, AFGC-ACI-fib-RILEM, Montpellier, France: 211-220.

Graybeal, B.A. 2008. Flexural Behavior of an Ultrahigh-Performance Concrete I-Girder. *Journal of Bridge Engineering*, **13**(6): 602-610.

Kim, D.J., Naaman, A.E. and El-Tawil, S. 2009. High Performance Fiber Reinforced Cement Composites with Innovative Slip Hardening Twisted Steel Fibers. *International Journal of Concrete Structures and Materials*, **3**(2): 119-126.

Wahba, Kirllos. 2012. Mechanical and Structural Properties of Ultra High Performance Fiber Reinforced Concrete. *Master's Thesis*, Ryerson University.

Maca, P., Radoslav, S. and Tomas, V. 2013. Experimental Investigation of Mechanical Properties of UHPFRC. *Procedia Engineering*, ASCE, **65**: 14-19.

Naaman, A.E. 2008. High Performance Fiber Reinforced Cement Composites: Classification and Applications. *International Workshop, High-Performance Construction Materials*, CBM-CI, Karachi, Pakistan: 389-401.

Othman, H. 2016. Performance of Ultra-High Performance Fiber Reinforced Concrete Plates Under Impact Loads. *Ph.D. Dissertation*, Ryerson University.

Othman, H. and Marzouk, H. 2016. Strain Rate Sensitivity of Fiber-Reinforced Cementitious Composites. *Materials Journal, ACI*, **113**(2): 143-150.

Othman, H. and Marzouk, H. 2018. Applicability of Damage Plasticity Constitutive Model for Ultra-High Performance Fibre-Reinforced Concrete Under Impact Loads. *International Journal of Impact Engineering*, **114**: 20-31.

Ozbakkaloglu, T. and Saatcioglu, M. 2004. Rectangular Stress Block for High-Strength Concrete. *Structural Journal*, ACI, **101**(4): 475-482.

Singh, M., Sheikh, A.H., Mohamed, M.S., Visintin, P. and Griffith, M.C. and Miller. 2017. Experimental and Numerical Study of the Flexural Behaviour of Ultra-High Performance Fibre Reinforced Concrete Beams. *Construction and Building Materials*, **138**: 12-25.

Wille, K., Kim, D.J. and Naaman, A.E. 2010. Strain-hardening UHP-FRC with Low Fiber Contents. *Materials and Structures*, **44**: 583-598.

Wille, K., Naaman, A.E., El-Tawil, S., and Parra-Montesinos, G.J. 2012. Ultra-High Performance Concrete and Fiber Reinforced Concrete: Achieving Strength and Ductility Without Heat Curing. *Materials and Structures*, **45**: 309-324.

Xu, M. and Wille, K. 2015. Fracture Energy of UHP-FRC Under Direct Tensile Loading Applied at Low Strain Rates. *Composites Part B: Engineering*, **80**: 116-125.

Yazdizadeh, Z. 2012. Use of Fiber Brag Gating Sensors in Civil Engineering Applications. *Master's Thesis*, Ryerson University.